Cyp2c70 is responsible for the species difference in bile acid metabolism between mice and humans

Takahashi, Shogo; Fukami, Tatsuki; Masuo, Yusuke; Brocker, Chad N.; Xie, Cen; Krausz, Kristopher W.

Published in:
Journal of Lipid Research

DOI:
10.1194/jlr.M071183

Publication date:
2016

Document Version
Peer reviewed version

Cyp2c70 is responsible for the species difference in bile acid metabolism between mice and humans

Shogo Takahashi[1], Tatsuki Fukami[1], Yusuke Masuo[1], Chad N. Brocker[1], Cen Xie[1], Kristopher W. Krausz[1], C. Roland Wolf[2], Colin J. Henderson[2], and Frank J. Gonzalez[1]

[1]Laboratory of Metabolism, National Cancer Institute, National Institutes of Health, Bethesda MD 20892, USA

[2]Division of Cancer, School of Medicine, Jacqui Wood Cancer Centre, University of Dundee, Ninewells Hospital, Dundee, DD1 9SY, United Kingdom.

Correspondence:

Frank J. Gonzalez

E-mail: gonzalef@mail.nih.gov

Tel: 301-496-9067

Running title: Cyp2c70 produces α-MCA and β-MCA

Abbreviations: 7-ER, 7-ethoxyresorufin; CA, cholic acids; CDCA, chenodeoxycholic acid; CYP, cytochrome P450; *Cyp1a*-null, *Cyp1a*-cluster null; *Cyp2c*-null, *Cyp2c*-cluster null; *Cyp2d*-null, *Cyp2d*-cluster null; *Cyp3a*-null, *Cyp3a*-cluster null; CYP7a1, cholesterol 7α-hydroxylase; FGF15, fibroblast growth factor 15; FXR, farnesoid X receptor; HBSS, Hank's buffered salt solution; h*CYP2C9*, *CYP2C9*-humanized; HDCA, hyodeoxycholic acid; LCA, lithocholic acid; α-MCA, α-muricholic acid; β-MCA, β-muricholic acid; PBS, phosphate-buffered saline; *Ppia*, peptidylprolyl isomerase A; T-α-MCA, tauro-α-muricholic acid ; T-β-MCA, tauro-β-muricholic acid; ω-MCA, ω-muricholic acid; T-CDCA, tauro-chenodeoxycholic acid; T-LCA, tauro-lithocholic acid; T-HDCA, tauro-hyodeoxycholic acid; T-UDCA, tauro-ursodeoxycholic acid; T-ω-MCA, tauro-ω-muricholic acid; UDCA, ursodeoxycholic acid.

Abstract

Bile acids are synthesized from cholesterol in the liver and subjected to multiple metabolic biotransformations in hepatocytes, including oxidation by cytochromes P450 (CYP)s and conjugation with taurine, glycine, glucuronic acid, and sulfate. Mice and rats can hydroxylate chenodeoxycholic acid (CDCA) at the 6β-position to form α-muricholic acid (α-MCA), and ursodeoxycholic acid (UDCA) to form β-muricholic acid (β-MCA). However, MCA is not formed in humans to any appreciable degree and the mechanism for this species difference is not known. Comparison of several *Cyp*-null mouse lines revealed that α-MCA and β-MCA were not detected in the liver samples from *Cyp2c*-cluster null (*Cyp2c*-null) mice. Global bile acids analysis further revealed the absence of MCA and their conjugated-derivatives, and high concentration of CDCA, UDCA in *Cyp2c*-null mouse cecum and feces. Analysis of recombinant CYPs revealed that α-MCA and β-MCA were produced by oxidation of CDCA and UDCA by Cyp2c70. *CYP2C9*-humanized mice have similar bile acid metabolites as the *Cyp2c*-null mice, indicating that human CYP2C9 does not oxidize CDCA and UDCA thus explaining the species differences in production of MCA. Since humans do not produce MCA, they lack tauro-β-MCA, a farnesoid X receptor (FXR) antagonists in mouse, that modulates obesity, insulin resistance and hepatosteatosis.

Supplementary key words: bile acid metabolism • chenodeoxycholic acid • cytochrome P450 • Cyp2c70 • enzyme kinetics • liver • muricholic acid • species difference • ursodeoxycholic acid

Introduction

Bile acids are synthesized from cholesterol in the liver and secreted through the biliary tract into the small intestine, where they aid in the absorption of lipids and fat-soluble vitamins (1, 2). Greater than 90% of bile acids produced in the liver are reabsorbed in the small intestine in the process of enterohepatic circulation. Bile acid synthesis and transport in the liver and intestine is regulated by the farnesoid X receptor (FXR, NR1H4), a member of the nuclear receptor superfamily (3, 4). Bile acids are subject to multiple metabolic biotransformations in hepatocytes, including conjugation with taurine, glycine, glucuronic acid, and sulfate (5). Mice and rats can hydroxylate chenodeoxycholic acid (CDCA) at the 6β-position to form α-muricholic acid (α-MCA), and ursodeoxycholic acid (UDCA) to form β-muricholic acid (β-MCA). MCA is produced in both mouse and rat liver, but is not formed at significant levels in human liver, thus indicating a species difference in MCA synthesis. In addition, mice mainly produce taurine conjugates of bile acids, while humans produce both mostly glycine conjugates and some taurine conjugates (6); rats also carry out both taurine and glycine conjugation. This is of particular interest since the taurine conjugate of β-MCA, T-β-MCA, is an antagonist of FXR in the ileum that controls FXR signaling and metabolic disease in mouse models of obesity (7-9).

While the hepatic cytochromes P450 (CYP) play a central role in the metabolism of drugs, toxins, and carcinogens, they also carry out key metabolic reactions in steroid hormone and bile acid synthesis. A number of CYPs participate in the synthesis of bile acid metabolites, with cholesterol 7α-hydroxylase (CYP7A1) generally considered the rate limiting enzyme in bile acid synthesis (10). Cyp7a1 is under control of FXR in the liver, and by FXR in the intestine through modulation of fibroblast growth factor 15 (FGF15) produced in the intestine that suppresses *Cyp7a1* expression in the liver (11). The mammalian CYPs have remarkable diversity between species, with 57 *CYP* genes identified in humans, and more than 100 putatively functional *Cyp* genes described in the mouse (12). For example, while the *CYP1A/Cyp1a* genes are conserved between mice and humans, the *CYP2C*, *CYP2D*, and *CYP3A* gene clusters have markedly diverged between the two species (13). To overcome the differences that exist in the substrate

specificity, and multiplicity of CYPs between species, significant efforts have been made to develop and characterize *Cyp*-null and *CYP*-humanized mice, with the aim to determine the metabolic functions of CYPs and to provide mouse models that better predict human pathways of metabolism (14, 15). Viable knockout models of the mouse *Cyp3a* (16, 17), *Cyp2d* (18), *Cyp1a* (19) and *Cyp2c* (20) gene clusters were described, which are associated with metabolic differences in the metabolism of xenobiotics as compared with wild-type controls.

In present study, *Cyp*-null mice were used to determine which CYPs are responsible for the differences in production of bile acid metabolites between humans and mice, notably the hepatic synthesis of MCA. Individual BA concentrations were determined in wild-type, *Cyp*-null mice leading to the identification of Cyp2c70 as the CYP responsible for MCA synthesis in mice. This was confirmed by recombinant Cyp2c70 expression and Cyp2c70 siRNA inhibition in primary mouse hepatocytes.

MATERIALS AND METHODS

Animal maintenance and treatments

All animal studies and procedure were carried out in accordance with Institute of Laboratory Animal Resources guidelines and approved by the National Cancer Institute Animal Care and Use Committee. Mice were housed in a pathogen-free animal facility under a standard 12-hour light/dark cycle and given pelleted NIH-31 chow diet and water ad libitum. Male mice between 8 and 12 weeks of age were used for isolation of primary hepatocytes and preparation of liver microsomes. Liver tissue, fecal samples and ileum/cecum contents for metabolomics analysis were collected in Dundee and shipped to the NCI for analysis. Adult *Cyp1a*-cluster null (*Cyp1a*-null) (19), *Cyp2c*-cluster null (*Cyp2c*-null) (20), *Cyp2d*-cluster null (*Cyp2d*-null)(18), *Cyp3a*-cluster null (*Cyp3a*-null) (16) and *CYP2C9*-humanized (h*CYP2C9*) (20) mice were housed singly in open-top cages with *ad libitum* 24 hours access to food and water. RM1A chow diet (Special Diets Services, Witham, UK) was removed for the final 4 hours before killing. After 24 hours, fecal pellets were collected, mixed and 500 mg snap-frozen and stored at -80°C. Mice were

killed by CO_2 asphyxiation and blood collected by cardiac puncture. Tissues were excised and immediately frozen in liquid nitrogen and serum and tissues were stored at -80°C until use.

Measurement of mRNAs

Total RNA of liver was extracted using TRIzol reagent (Thermo Fisher Scientific, Waltham, MA). qPCR was performed using cDNA generated from 1 µg total RNA with qScript™ cDNA SuperMix (Quanta Biosciences, Gaithersburg, MD). qPCR reactions were carried out using SYBR green qPCR master mix (Biotools, Houston, TX) in an QuanStudio™ 7 Flex System. The primer pairs were designed using Primer-BLAST (National Center for Biotechnology Information), and was shown in Supplementary Table 1. Values were quantified with the comparative CT method and normalized to peptidylprolyl isomerase A (Ppia).

Quantification of bile acid metabolites

Twenty mg of liver, cecum and feces were homogenized with 200 µL of 100% acetonitrile containing 1 µM d5-taurocholate (Sigma-Aldrich) as an internal standard and centrifuged twice at 15,000 × g for 25 minutes at 4°C for removal of precipitated proteins and other particulates. The supernatant was diluted by an equal volume of HPLC grade water (Thermo Fisher Scientific, Waltham, MA) containing 0.1% formic acid. Quantification of bile acid metabolites were measured as described previously (7, 9). LC-MS was performed on a Waters Acquity H-Class UPLC system using a Waters Acquity BEH C18 column (2.1 × 100 mm) coupled to a Waters Xevo G2 QTOFMS. UPLC was performed by the following protocol: A, 0.1% Formic acid in water and B, 0.1% formic acid in acetonitrile. An initial gradient of 80% A for 4 minutes, to 60% A at 15 minutes, to 40% A at 20 minutes, to 10% A at 21 minutes, followed by flushing for 1 minute, then equilibration under the initial conditions for 4 minutes. The flow rate was 0.4 ml/minute, and the column temperature was maintained at 45°C. A Waters Xevo G2 QTOF was operated in negative mode, scanning *m/z* 50-1200 at a rate of 0.3 seconds/scan. The following instrument conditions were used: 1.5 kV capillary voltage, 150°C source temperature, 30 V sampling cove, and a

desolvation gas flow rate of 850 L/hour at 500°C. The chromatograms showing the separation of the various bile acid isomers is included in Supplemental Fig. S1 and S2.

CDCA and UDCA oxidation activity

The CDCA and UDCA oxidation was determined as follows. A typical incubation mixture (final volume of 0.1 ml) contained 100 mM potassium phosphate buffer, pH 7.4, and various enzyme sources (0.4 mg/ml mouse microsomal protein, 1.0 mg/ml S9 from liver tissues of *Cyp2c*-null, *Cyp3a*-null and wild-type mice). In a preliminary study, the rate of formation of α-MCA and β-MCA was found to be linear with respect to the protein concentrations (up to 0.5 mg/ml mouse microsomal protein and incubation time for 30 min). Chenodeoxycholic acid-2, 2, 4, 4-d4 (CDCA-d4, Toronto Research Chemicals, Inc., Toronto, Canada), ursodeoxycholic acid-2, 2, 4, 4-d4, (UDCA-d4, Cambridge Isotope Laboratories, Inc., Andover, MA) and 7-ethoxyresorufin (7-ER, Sigma-Aldrich) were dissolved in dimethyl sulfoxide (DMSO), and the final concentration of DMSO in the incubation mixture was 0.1%. The reaction was initiated by the addition of 4 to 100 μM CDCA, 40 to 1000 μM UDCA, and 1 μM 7-ER, after 7-min pre-incubation at 37°C. Following a 20-min incubation at 37°C, the reaction was terminated by the addition of 0.1 ml of ice-cold acetonitrile. After removal of the protein by centrifugation at 15000g, 4℃, 15 min, an equal volume of HPLC grade water containing 0.1% formic acid was added followed by centrifugation at 15000g, 4℃, 15 min. 10 μL of the supernatant was subjected to UPLC-QTOFMS. The ions for α-MCA-d4 and β-MCA-d4 are *m/z* 411.3069 in the negative ion mode.

Transfection of plasmids expressing mouse Cyp2c29 and Cyp2c70.

HepG2 cells were maintained in RPMI 1640 medium with L-glutamine containing 10% fetal bovine serum with 5% CO_2 at 37°C. The cells were transfected in 12-well plate with 1 μg of Cyp2c29 expression vector (MGC premier Expression-Ready cDNA clone for *Cyp2c29* - pCS6, BC019908, transOMIC

technologies, Huntsville, AL), Cyp2c70 expression vector (MGC premier Expression-Ready cDNA clone for *Cyp2c70* - pCS6, BC016494, transOMIC technologies) and mock vector using Lipofectamine 3000 (Thermo Fisher Scientific). After incubation for 48 hours, the cells were treated with 25 μM CDCA-d4 or 400 μM UDCA-d4.

Preparation and treatment of mouse primary hepatocytes.

Primary hepatocytes were isolated from C57BL/6J mice as described previously (21). Briefly, after killing mice by CO_2 asphyxiation, the abdomen was incised and mesentery and intestine moved to expose the portal vein. A cannula was inserted into the portal vein and liver was perfused with 40 ml of Hank's buffered salt solution (HBSS) without magnesium or calcium (Thermo Fisher Scientific) containing 1 mM EDTA at 4 ml/min. Blood was extravasated by cutting the inferior vena cava. After perfusion of the entire liver using 50 ml of HBSS containing collagenase I and II (0.6 mg/ml each, Thermo Fisher Scientific) and calcium chloride dehydrate (5 mM) at the speed of 4 ml/min, the digested liver was removed and placed in a sterile 10-cm Petri dish with 10 mM phosphate-buffered saline (PBS). The hepatic capsule was torn by fine-tip forceps and dispersed cells were filtered through 70-μm cell strainer (Becton Dickinson and Company) into a 50-ml tube and centrifuged at 200 × g, at 4 °C for 2 minutes. Hepatocytes were further washed and purified by gradient centrifugation using Percoll Plus (GE Healthcare, Buckinghamshire, UK). After washing with HBSS and trypan blue staining, the number of hepatocytes were counted and then seeded in collagen-coated 12-well plates (Becton Dickinson and Company) at a density of 4×10^5 cells/well. Primary hepatocytes were cultured in William's E medium (Thermo Fisher Scientific) with 10% fetal bovine serum, and antibiotics (100 U/ml penicillin and 100 μg/ml streptomycin). Four-to six hours after seeding, the cells were treated with 10 nM Cyp2c29 Silencer® Select Pre-designed siRNA (Thermo Fisher Scientific), Cyp2c70 Silencer® Select Pre-designed siRNA (Thermo Fisher Scientific), and Silencer® Select Negative Control #1 (Thermo Fisher Scientific) using Lipofectamine® RNAiMAX (Thermo Fisher Scientific). Twenty-four hours after siRNA treatment, the cells were treated with medium containing CDCA-d4 or UDCA-d4 for 4 hours. At the prescribed time

points, medium and cells were harvested and subjected to measurement bile acids using QTOF-MS and qPCR respectively.

Statistical Analysis.

Statistical analysis was performed with Prism version 6 (GraphPad Software). Appropriate statistical analysis was applied, assuming a normal sample distribution. When comparing two groups, statistical significance was determined using two-tailed Student's t-test. When more than two groups were investigated, one-way ANOVA followed by Tukey's *post-hoc* correction was applied for comparisons. A *p* value of less than 0.05 was considered as significant difference. Results are expressed as the mean value and SD values.

RESULTS

MCA and conjugated-MCA in the liver of *Cyp*-null mice

To determine the influence of CYPs on the formation of α-MCA and β-MCA, bile acids were measured in livers of *Cyp1a*-null, *Cyp2c*-null, *Cyp2d*-null and *Cyp3a*-null mice. α-MCA and β-MCA were not detected in livers from *Cyp2c*-null mice, although they were present in other *Cyp*-null mouse lines (Figure 1A). Moreover, T-α-MCA and T-β-MCA were also not detected in *Cyp2c*-null mouse livers (Figure 1B). These results suggest that mouse Cyp2c might produce α-MCA and β-MCA.

Kinetic analysis of MCA production *in vitro*

To investigate MCA production from CDCA and UDCA, the activities of α-MCA and β-MCA production were measured using liver S9 fractions of wild-type, *Cyp2c*-null, and *Cyp3a*-null mice at 50 μM CDCA-d4 or 500 μM UDCA-d4 (Figure 2A, 2B). α-MCA-d4 was detected in CDCA-d4-treated S9 from wild-type and *Cyp3a*-null mice, but was not detected in S9 from *Cyp2c*-null mice (Figure 2A). β-MCA-d4 was not detected in any of the CDCA-d4-treated groups. α-MCA-d4 was not detected in the

UDCA-d4 treated-group while β-MCA was detected in S9 from wild-type and *Cyp3a*-null mice but was undetected in *Cyp2c*-null mice (Figure 2B). As a control, it was confirmed that liver S9 fractions from all of mouse lines showed the 7-ethoxyresorufin (7-ER) *O*-deethylase activity, which is a marker activity of mouse Cyp1a2 (Figure 2C). Kinetic analyses using different concentrations of CDCA and UDCA were performed using liver microsomes to determine the Km and Vmax values for α-MCA and β-MCA productions from CDCA and UDCA, respectively. The Km and Vmax values for α-MCA production were 8.19 ± 0.24 μM and 0.58 ± 0.01 nmol/min/mg, and those for β-MCA production were 321 ± 46 μM and 0.418 ± 0.03 nmol/min/mg, respectively (Figure 2D). These data indicate that the catalytic efficiency for α-MCA production is higher than that for β-MCA production.

Levels of individual *Cyp2c* mRNAs in wild-type mice

There are 16 kinds of *Cyp2c* genes in mice, including *Cyp2c53* that is a pseudogene, and their proteins are mainly expressed in the liver. The expression of each *Cyp2c* mRNA in liver was determined by RT-qPCR. The levels of *Cyp2c29, Cyp2c50, Cyp2c67, Cyp2c69*, and *Cyp2c70* mRNAs were 5.3-, 1.8-, 3.0-, 1.5- and 1.9-fold that of Cyp2c44 mRNA, which is the only *Cyp2c* gene not deleted in the *Cyp2c*-null mice (Figure 3). The mouse *Cyp2c* cluster, with the exception of *Cyp2c44*, which is located 4 Mb away from the main *Cyp2c* gene cluster, was flanked with Cre recombinase recognition (loxP) sites using two consecutive rounds of targeting in mouse ES cells (20).

CDCA and UDCA oxidation activity by recombinant mouse Cyp2c70

To investigate which mouse Cyp2c isoform produces α-MCA from CDCA, Cyp2c29 and Cyp2c70 were transiently expressed in HepG2 cells as revealed by mRNA expression (Figure 4A). Recombinant Cyp2c29 and Cyp2c70 showed the production of α-MCA-d4 from CDCA was only detected in cells expressing Cyp2c70. β-MCA was not detected in these groups (Figure 4B). In contrast, α-MCA-d4 was

not detected when UDCA-d4 was used as a substrate. Cyp2c70-expressing cells also showed β-MCA production from UDCA (Figure 4C). These results suggest that Cyp2c70 catalyzes CDCA and UDCA oxidations to α-MCA and β-MCA, respectively.

Knockdown of Cyp2c70 reduces MCA production in mouse primary hepatocytes

To further confirm whether Cyp2c70 produces MCA from CDCA or UDCA, siRNA against Cyp2c29 (Si-Cyp2c29) and Cyp2c70 (Si-Cyp2c70) were transfected to mouse primary hepatocytes. Si-Cyp2c29 and si-Cyp2c70 significantly decreased *Cyp2c29* and *Cyp2c70* mRNA levels, respectively, and did not affect *Cyp2c44* mRNA expression (Figure 5A). In the presence of CDCA, α-MCA levels were specifically decreased in the si-Cyp2c70-treated cells, while β-MCA production was lowered in mouse primary hepatocytes in the presence of UDCA. This result reveals that Cyp2c70 is responsible for MCA production from CDCA and UDCA in mouse liver.

Bile acids in the liver, cecum and feces from *Cyp2c*-null mice and *CYP2C9*-humanized mice

To determine the consequence of loss of Cyp2c70 in the *Cyp2c*-null and *CYP2C9*-humanized mice, bile acids were measured in liver, cecum and feces of wild-type, *Cyp2c*-null, and *CYP2C9*-humanized mice. h*CYP2C9* mice were generated from the *Cyp2c*-deleted ES cells described above by further Cre-mediated insertion of an expression cassette in which the human *CYP2C9* gene is under control of the liver-specific mouse albumin promoter (20). In this study, the *CYP2C9*-humanized mice were used for the human model, because among human CYP2C enzymes, CYP2C9 is most abundant in the liver and is involved in the metabolism of various kinds of endogenous and exogenous compounds. α-MCA and β-MCA and their taurine conjugates were not detected in the liver, cecum and feces of *Cyp2c*-null and *CYP2C9*-humanized mice (Figure 6). Moreover, the contents of CDCA and UDCA, which are precursor substances of α-MCA and β-MCA in mice, respectively, in *Cyp2c*-null and *CYP2C9*-humanized mice

were significantly higher than those in wild-type mice. The contents of T-CDCA and T-UDCA were also high in *Cyp2c*-null and *CYP2C9*-humanized mice. In cecum and feces, lithocholic acid (LCA) was also significantly highly detected in *Cyp2c*-null and *CYP2C9*-humanized mice as compared with wild-type mice. In addition, tauro-LCA (T-LCA) was highly detected in these mice.

DISCUSSION

An earlier study revealed that mice with hepatocyte-specific deletion of NADPH–cytochrome P450 reductase (22), which decreased all CYPs activities, were found to have marked differences in a bile acid compositions including lower MCA and taurine-conjugated MCA as compared to their wild-type counterparts (23). However, this study could not distinguish which CYP isoform produced MCA. The current work demonstrated that mouse *Cyp2c70* is responsible for production of MCA from CDCA or UDCA. *Cyp2c*-null mice and *CYP2C9*-humanized mice did not produce any MCA, in contrast to wild-type mice and mouse lines lacking expression of Cyp1a, Cyp2d and Cyp3a isoform. *Cyp2c*-null mice also have high concentration of CDCA and UDCA (and their taurine conjugates), the substrates for α-MCA and β-MCA, respectively.

LCA is produced from CDCA in the human and mouse large intestine. LCA is present in only trace levels in mouse liver, likely due to the low concentrations of CDCA. LCA and T-LCA, which are present in very low levels in wild-type mice, were found at significant concentrations in *Cyp2c*-null and *CYP2C9*-humanized mouse livers. The hepatic *Cyp7a1* and *Cyp8b1* mRNA levels were not significantly different between wild-type, *Cyp2c*-null and h*CYP2C9* mice (Supplemental Fig. S3). The increased concentrations of CDCA in livers of *Cyp2c*-null mice led to the production of LCA through a 7-dehydroxylation reaction by gut bacteria (24). LCA is then reabsorbed to the liver where it is conjugated with taurine. This is of particular interest, since LCA is considered a toxic bile acid (25). Thus, the lack of MCA production indirectly causes an increase in LCA. However, LCA is efficiently conjugated in mice leading to decreased potential for hepatotoxicity. Indeed, the homozygous *CYP2C9*-humanized and *Cyp2c*-null mice appeared normal, could not be distinguished from wild-type mice, they had normal body weights, liver

weights, and fertility (Supplemental Fig. S4A). The *Cyp2c*-null mice show no evidence for liver damage as compared to wild-type mice, although an increase in ALT and AST was observed in some mice due to inter-animal variability this change was not significant. The only significant phenotypic change in the *CYP2C9*-humanized mice was a decrease in alkaline phosphatase activity, while the *Cyp2c*-null mice exhibited a similar change and a small but significant decrease in plasma high-density lipoprotein and cholesterol (20).

T-β-MCA was identified as a potent FXR antagonist in mice (9, 26). Inhibition of intestinal FXR resulted in the alleviation of metabolic disease including obesity, insulin resistance and hepatic steatosis (7-9). However, the question arises whether humans bile acids would have similar effects on FXR since humans do not produce MCA and thus T-β-MCA due to a lack of a CYP2C enzyme activity similar to mouse Cyp2c70. It is also noteworthy that UDCA is elevated in the *Cyp2c*-null mice and shows potential FXR antagonist activity in humans (27). FXR signaling in mice is dependent on the relative local concentration of endogenous agonist and antagonist that result from bile acid metabolism in the liver and intestine. Body weights and hepatic lipid concentrations (triglyceride, total cholesterol, phospholipid and non-esterified fatty acid) were not significant changed in wild-type, *Cyp2c*-null and h*CYP2C9* mice (Supplemental Fig. S4B). The impact of these changes on the susceptibility to metabolic disease in the *Cyp2c*-null mice is an area of great interest and will require analysis of high-fat diet-induced obesity, insulin resistance and fatty livers (7, 9).

The mouse and the human *CYP2C* cluster differ significantly in their genomic organization, with 15 functional genes described in mice compared with only four genes in humans. Analysis of hepatic mRNAs revealed that *Cyp2c29* is the most abundant while *Cyp2c50*, *Cyp2c67*, *Cyp2c69*, and *Cyp2c70* mRNAs were expressed at similar levels (12). Humans do not have an obvious homolog of Cyp2c70, at least at the level of primary amino acid sequence comparison (CYP2C8. 76%; CYP2C9, 79%; CYP2C18, 79%; CYP2C19, 79%).However, there is significant protein homology between Cyp2c70 and CYP2C22 which is the rat homolog of Cyp2c70 (Table 1). This is noteworthy because rats also have MCA similar to

mice (28). Murine *Cyp2c37/38/39* and *Cyp2c40* genes are endogenous female specific *Cyp2c* genes. However, a much smaller gender difference in expression characterized Cyp2c29 and Cyp2c70 when comparing wild-type males and wild-type females (29). These findings support the view that Cyp2c70 is a primary enzyme responsible for MCA production. No other specific substrates for Cyp2c70 have been reported.

In mice, β-MCA and T-β-MCA appear to be more abundant than α-MCA and T-α-MCA. However, kinetic studies revealed a higher affinity of Cyp2c70 for CDCA than UDCA. These results suggest that α-MCA production is higher than that of β-MCA due to increased catalytic efficiency toward CDCA in mouse. The microbiota is involved in the metabolism of bile acids, particularly dehydroxylation and deconjugation reactions (9, 30, 31). Epimerization from α-MCA to β-MCA might occur in mouse intestine by microbiome metabolism through enzymes other than CYPs. Oxidation and epimerization of the 7-hydroxy groups of bile acids in the intestine are carried out by hydroxysteroid dehydrogenase expressed by intestinal bacteria (32).

Some studies have investigated whether bile acid concentrations might be useful to differentiate among various liver diseases (33-35). Bile acids also act agonists or antagonists for nuclear receptor such as FXR, pregnane X receptor (NR1I2), vitamin D receptor (NR1I1) and the G protein-coupled bile acid receptor, TGR5 (36). However, it is known that bile salt composition markedly differs between various species (37). As noted above, T-β-MCA is an FXR antagonist in mouse intestine, but humans do not produce MCA (26).

In addition, humans make glycine conjugates of bile acids while mice only make taurine conjugates. Thus, mice are a poor model to investigate and predict the influence of bile acid metabolites in human disease. Mice lacking expression of the *Cyp2c* cluster showed similar bile acids profiling to humans, but still made taurine conjugates. Perhaps humanizing the bile acid conjugating enzymes bile acid-CoA ligase and bile acid-CoA:amino acid *N*-acyltransferase would make a more complete bile acid-humanized mouse line. Further, the bile acid profiles indicate that the gut microbiota of the *Cyp2c*-null mice may not

optimally hydrolyze the taurine conjugates of CDCA and LCA since T-CDCA and T-LCA accumulate in the cecum and feces. Since mouse gut microbiota seldom encounter these conjugates, the *Cyp2c*-null mice may not be an accurate model for human bile acid metabolism. Therefore, a mouse model that is optimal to study human diseases related to bile acids may have to be colonized with human gut microbiota. Taken together, the present study revealed that Cyp2c70 is the principal enzyme involved in MCA production and is responsible for the differences in bile acid metabolite profile between humans and mice.

Acknowledgments

The authors wish to acknowledge the assistance of Julia Carr, Aileen McLaren and Tania Frangova for performing the animal studies in University of Dundee. This work was supported by the National Cancer Institute Intramural Research Program, Center for Cancer Research and U54 ES16015 (F.J.G) and a Programme Grant support from Cancer Research UK, C4639/A10822 to CRW. ST was supported by a Japanese Society for the Promotion of Science Research Fellowship for Japanese Biomedical and Behavioral Researcher at NIH (KAITOKU-NIH). FT and YM were supported by program for Advancing Strategic International Networks to Accelerate the Circulation of Talented Researchers (No. S2601) from the Japanese Society for the Promotion of Sciences.

REFERENCES

1. Russell, D. W. 2003. The enzymes, regulation, and genetics of bile acid synthesis. *Annu. Rev. Biochem.* **72**: 137-174.
2. Hofmann, A. F. 2009. The enterohepatic circulation of bile acids in mammals: form and functions. *Front Biosci (Landmark Ed)* **14**: 2584-2598.
3. Matsubara, T., F. Li, and F. J. Gonzalez. 2013. FXR signaling in the enterohepatic system. *Mol. Cell. Endocrinol.* **368**: 17-29.
4. Gonzalez, F. J. 2012. Nuclear receptor control of enterohepatic circulation. *Compr Physiol* **2**: 2811-2828.
5. Deo, A. K., and S. M. Bandiera. 2008. Identification of human hepatic cytochrome p450 enzymes involved in the biotransformation of cholic and chenodeoxycholic acid. *Drug Metab Dispos* **36**: 1983-1991.
6. Hardison, W. G. 1978. Hepatic taurine concentration and dietary taurine as regulators of bile acid conjugation with taurine. *Gastroenterology* **75**: 71-75.
7. Jiang, C., C. Xie, F. Li, L. Zhang, R. G. Nichols, K. W. Krausz, J. Cai, Y. Qi, Z. Z. Fang, S. Takahashi, N. Tanaka, D. Desai, S. G. Amin, I. Albert, A. D. Patterson, and F. J. Gonzalez. 2015. Intestinal farnesoid X receptor signaling promotes nonalcoholic fatty liver disease. *J Clin Invest* **125**: 386-402.
8. Jiang, C., C. Xie, Y. Lv, J. Li, K. W. Krausz, J. Shi, C. N. Brocker, D. Desai, S. G. Amin, W. H. Bisson, Y. Liu, O. Gavrilova, A. D. Patterson, and F. J. Gonzalez. 2015. Intestine-selective farnesoid X receptor inhibition improves obesity-related metabolic dysfunction. *Nat Commun* **6**: 10166.
9. Li, F., C. Jiang, K. W. Krausz, Y. Li, I. Albert, H. Hao, K. M. Fabre, J. B. Mitchell, A. D. Patterson, and F. J. Gonzalez. 2013. Microbiome remodelling leads to inhibition of intestinal farnesoid X receptor signalling and decreased obesity. *Nat Commun* **4**: 2384.
10. Russell, D. W., and K. D. Setchell. 1992. Bile acid biosynthesis. *Biochemistry* **31**: 4737-4749.
11. Inagaki, T., M. Choi, A. Moschetta, L. Peng, C. L. Cummins, J. G. McDonald, G. Luo, S. A. Jones, B. Goodwin, J. A. Richardson, R. D. Gerard, J. J. Repa, D. J. Mangelsdorf, and S. A. Kliewer. 2005. Fibroblast growth factor 15 functions as an enterohepatic signal to regulate bile acid homeostasis. *Cell Metab.* **2**: 217-225.
12. Nelson, D. R., D. C. Zeldin, S. M. Hoffman, L. J. Maltais, H. M. Wain, and D. W. Nebert. 2004. Comparison of cytochrome P450 (CYP) genes from the mouse and human genomes, including nomenclature recommendations for genes, pseudogenes and alternative-splice variants. *Pharmacogenetics* **14**: 1-18.
13. Scheer, N., L. A. McLaughlin, A. Rode, A. K. Macleod, C. J. Henderson, and C. R. Wolf. 2014. Deletion of 30 murine cytochrome p450 genes results in viable mice with compromised drug metabolism. *Drug Metab Dispos* **42**: 1022-1030.
14. Cheung, C., and F. J. Gonzalez. 2008. Humanized mouse lines and their application for prediction of human drug metabolism and toxicological risk assessment. *J. Pharmacol. Exp. Ther.* **327**: 288-299.
15. Scheer, N., and C. R. Wolf. 2014. Genetically humanized mouse models of drug metabolizing enzymes and transporters and their applications. *Xenobiotica* **44**: 96-108.
16. van Herwaarden, A. E., E. Wagenaar, C. M. van der Kruijssen, R. A. van Waterschoot, J. W. Smit, J. Y. Song, M. A. van der Valk, O. van Tellingen, J. W. van der Hoorn, H. Rosing, J. H. Beijnen, and A. H. Schinkel. 2007. Knockout of cytochrome P450 3A yields new mouse models for understanding xenobiotic metabolism. *J Clin Invest* **117**: 3583-3592.
17. Hasegawa, M., Y. Kapelyukh, H. Tahara, J. Seibler, A. Rode, S. Krueger, D. N. Lee, C. R. Wolf, and N. Scheer. 2011. Quantitative prediction of human pregnane X receptor and cytochrome P450 3A4 mediated drug-drug interaction in a novel multiple humanized mouse line. *Mol. Pharmacol.* **80**: 518-528.

18. Scheer, N., Y. Kapelyukh, J. McEwan, V. Beuger, L. A. Stanley, A. Rode, and C. R. Wolf. 2012. Modeling human cytochrome P450 2D6 metabolism and drug-drug interaction by a novel panel of knockout and humanized mouse lines. *Mol. Pharmacol.* **81**: 63-72.
19. Dragin, N., S. Uno, B. Wang, T. P. Dalton, and D. W. Nebert. 2007. Generation of 'humanized' hCYP1A1_1A2_Cyp1a1/1a2(-/-) mouse line. *Biochem. Biophys. Res. Commun.* **359**: 635-642.
20. Scheer, N., Y. Kapelyukh, L. Chatham, A. Rode, S. Buechel, and C. R. Wolf. 2012. Generation and characterization of novel cytochrome P450 Cyp2c gene cluster knockout and CYP2C9 humanized mouse lines. *Mol. Pharmacol.* **82**: 1022-1029.
21. Tanaka, N., S. Takahashi, Y. Zhang, K. W. Krausz, P. B. Smith, A. D. Patterson, and F. J. Gonzalez. 2015. Role of fibroblast growth factor 21 in the early stage of NASH induced by methionine- and choline-deficient diet. *Biochimica et biophysica acta* **1852**: 1242-1252.
22. Gu, J., Y. Weng, Q. Y. Zhang, H. Cui, M. Behr, L. Wu, W. Yang, L. Zhang, and X. Ding. 2003. Liver-specific deletion of the NADPH-cytochrome P450 reductase gene: impact on plasma cholesterol homeostasis and the function and regulation of microsomal cytochrome P450 and heme oxygenase. *J. Biol. Chem.* **278**: 25895-25901.
23. Cheng, X., Y. Zhang, and C. D. Klaassen. 2014. Decreased bile-acid synthesis in livers of hepatocyte-conditional NADPH-cytochrome P450 reductase-null mice results in increased bile acids in serum. *J. Pharmacol. Exp. Ther.* **351**: 105-113.
24. Fedorowski, T., G. Salen, G. S. Tint, and E. Mosbach. 1979. Transformation of chenodeoxycholic acid and ursodeoxycholic acid by human intestinal bacteria. *Gastroenterology* **77**: 1068-1073.
25. Hofmann, A. F. 2004. Detoxification of lithocholic acid, a toxic bile acid: relevance to drug hepatotoxicity. *Drug Metab. Rev.* **36**: 703-722.
26. Sayin, S. I., A. Wahlstrom, J. Felin, S. Jantti, H. U. Marschall, K. Bamberg, B. Angelin, T. Hyotylainen, M. Oresic, and F. Backhed. 2013. Gut microbiota regulates bile acid metabolism by reducing the levels of tauro-beta-muricholic acid, a naturally occurring FXR antagonist. *Cell Metab.* **17**: 225-235.
27. Mueller, M., A. Thorell, T. Claudel, P. Jha, H. Koefeler, C. Lackner, B. Hoesel, G. Fauler, T. Stojakovic, C. Einarsson, H. U. Marschall, and M. Trauner. 2015. Ursodeoxycholic acid exerts farnesoid X receptor-antagonistic effects on bile acid and lipid metabolism in morbid obesity. *Journal of hepatology* **62**: 1398-1404.
28. Katagiri, K., T. Nakai, M. Hoshino, T. Hayakawa, H. Ohnishi, Y. Okayama, T. Yamada, T. Ohiwa, M. Miyaji, and T. Takeuchi. 1992. Tauro-beta-muricholate preserves choleresis and prevents taurocholate-induced cholestasis in colchicine-treated rat liver. *Gastroenterology* **102**: 1660-1667.
29. Lofgren, S., R. M. Baldwin, M. Carleros, Y. Terelius, R. Fransson-Steen, J. Mwinyi, D. J. Waxman, and M. Ingelman-Sundberg. 2009. Regulation of human CYP2C18 and CYP2C19 in transgenic mice: influence of castration, testosterone, and growth hormone. *Drug Metab Dispos* **37**: 1505-1512.
30. Greathouse, K. L., C. C. Harris, and S. J. Bultman. 2015. Dysfunctional families: Clostridium scindens and secondary bile acids inhibit the growth of Clostridium difficile. *Cell Metab.* **21**: 9-10.
31. Buffie, C. G., V. Bucci, R. R. Stein, P. T. McKenney, L. Ling, A. Gobourne, D. No, H. Liu, M. Kinnebrew, A. Viale, E. Littmann, M. R. van den Brink, R. R. Jenq, Y. Taur, C. Sander, J. R. Cross, N. C. Toussaint, J. B. Xavier, and E. G. Pamer. 2015. Precision microbiome reconstitution restores bile acid mediated resistance to Clostridium difficile. *Nature* **517**: 205-208.
32. Hirano, S., and N. Masuda. 1981. Epimerization of the 7-hydroxy group of bile acids by the combination of two kinds of microorganisms with 7 alpha- and 7 beta-hydroxysteroid dehydrogenase activity, respectively. *J. Lipid Res.* **22**: 1060-1068.
33. de Aguiar Vallim, T. Q., E. J. Tarling, H. Ahn, L. R. Hagey, C. E. Romanoski, R. G. Lee, M. J. Graham, H. Motohashi, M. Yamamoto, and P. A. Edwards. 2015. MAFG is a transcriptional repressor of bile acid synthesis and metabolism. *Cell Metab.* **21**: 298-310.
34. Seeley, R. J., A. P. Chambers, and D. A. Sandoval. 2015. The role of gut adaptation in the potent effects of multiple bariatric surgeries on obesity and diabetes. *Cell Metab.* **21**: 369-378.

35. Jones, R. D., A. M. Lopez, E. Y. Tong, K. S. Posey, J. C. Chuang, J. J. Repa, and S. D. Turley. 2015. Impact of physiological levels of chenodeoxycholic acid supplementation on intestinal and hepatic bile acid and cholesterol metabolism in Cyp7a1-deficient mice. *Steroids* **93**: 87-95.
36. Thomas, C., A. Gioiello, L. Noriega, A. Strehle, J. Oury, G. Rizzo, A. Macchiarulo, H. Yamamoto, C. Mataki, M. Pruzanski, R. Pellicciari, J. Auwerx, and K. Schoonjans. 2009. TGR5-mediated bile acid sensing controls glucose homeostasis. *Cell Metab.* **10**: 167-177.
37. Botham, K. M., and G. S. Boyd. 1983. The metabolism of chenodeoxycholic acid to beta-muricholic acid in rat liver. *Eur. J. Biochem.* **134**: 191-196.

Table 1. Primary amino acid sequence comparison between mouse Cyp2c and human CYP2C

Mouse	Protein homology (%)	Human
Cyp2c29	83	CYP2C8
Cyp2c37	-	-
Cyp2c38	84	CYP2C8
Cyp2c39	73	CYP2C8
Cyp2c40	-	-
Cyp2c44	-	-
Cyp2c50	-	-
Cyp2c54	-	-
Cyp2c55	88	CYP2C18
Cyp2c65	86	CYP2C9
Cyp2c66	85	CYP2C9
Cyp2c67	-	-
Cyp2c68	-	-
Cyp2c69	-	-
Cyp2c70	-	-

Table 2. Primary amino acid sequence comparison between mouse Cyp2c and rat CYP2C

Mouse	Protein homology (%)	Rat
Cyp2c29	82	CYP2C7
Cyp2c37	-	-
Cyp2c38	82	CYP2C7
Cyp2c39	82	CYP2C7
Cyp2c40	-	-
Cyp2c44	95	CYP2C23
Cyp2c50	-	-
Cyp2c54	-	-
Cyp2c55	95	CYP2C24
Cyp2c65	84	CYP2C11
Cyp2c66	84	CYP2C11
Cyp2c67	-	-
Cyp2c68	-	-
Cyp2c69	-	-
Cyp2c70	94	CYP2C22

FIGURE LEGENDS

Fig. 1. Determination of MCA in various *Cyp*-null mice. Concentrations of MCA and conjugated-MCA in the liver extracts from *Cyp1a*-, *Cyp2c*-, *Cyp2d*-, *Cyp3a*- and wild-type mice. The mice, on a RM1A chow diet, were killed in the late morning after a 4 h fast. (A) α-MCA and β-MCA in liver samples. (B) T-α-MCA and T-ß-MCA in liver samples. Data are presented as the mean ± S. D. (n = 4-5).

Fig. 2. Kinetic analyses of MCA oxidation activities in mouse liver S9 and microsomes. (A) α-MCA-d4 and β-MCA-d4 production from CDCA-d4 by liver S9 from *Cyp2c*-, *Cyp3a*-null mice and wild-type (WT) mice. (B) α-MCA-d4 and β-MCA-d4 production from UDCA-d4 by liver S9 from *Cyp2c*-, *Cyp3a*-null mice and WT mice. (C) Resorufin production from 7-ethoxyresorufin by liver S9 from *Cyp2c*-, *Cyp3a*-null mice and WT mice. (D) Kinetics of α-MCA-d4 and β-MCA-d4 production from CDCA-d4 and UDCA-d4 by mouse liver microsomes, respectively. The kinetic parameters were estimated from the fitted curve using the computer program GraphPad Prism designed for nonlinear regression analysis. Each data point represents the mean ± S.D. of triplicate determinations.

Fig 3. Expression levels of mouse *Cyp2c* mRNA. Relative mRNA expression levels of mouse *Cyp2c* mRNAs in liver were determined by RT-qPCR analysis. Levels are relative to *Cyp2c44* mRNA. Each column represents the mean ± S.D. (n = 5).

Fig. 4. MCA production in HepG2 cells expressing recombinant Cyp2c70**.** (A) *Cyp2c29* and *Cyp2c70* mRNA levels in HepG2 cells transfected with Cyp expression vectors. (B) α-MCA-d4 and ß-MCA-d4 production in HepG2 cells transfected with Cyp2c29 and Cyp2c70 expression vectors Cells were incubated with 50 µM CDCA-d4. (C) α-MCA-d4 and β-MCA-d4 production in n HepG2 cells transfected with Cyp2c29 and Cyp2c70 expression vectors. Cells were incubated with 500 µM UDCA-d4. Data are presented as the mean ± S. D. (n = 3).

Fig. 5. MCA production in siRNA for Cyp2c70-transfected mouse primary hepatocytes. (A) *Cyp2c29* and *Cyp2c70* mRNA levels in mouse primary hepatocytes transfected with siRNAs against Cyp2c29 (Si-Cyp2c29) and Cyp2c70 (Si-Cyp2c70). (B) α-MCA-d4 and β-MCA-d4 production in mouse primary hepatocytes transfected with Si-Cyp2c29 and Si-Cyp2c70. Hepatocytes were incubated with 50 μM CDCA-d4. (C) α-MCA-d4 and β-MCA-d4 production in mouse primary hepatocytes transfected with Si-Cyp2c29 and Si-Cyp2c70. Hepatocytes were incubated with 500 μM UDCA-d4. Data are presented as the mean ± S. D. (n = 3).

Fig. 6. Bile acids profile in the liver, cecum, and feces from wild-type, *Cyp2c*-null mice and *CYP2C9*-humanized mice. (A) Unconjugated-bile acids and taurine-conjugated-bile acids in liver samples of *Cyp2c*-null mice, *CYP2C9*-humanized (h*CYP2C9*), and wild-type (WT) mice. (B) Unconjugated-bile acids and taurine-conjugated-bile acids in cecum samples of *Cyp2c*-null mice, h*CYP2C9*, and wild-type mice. (C) Unconjugated-bile acids and taurine-conjugated-bile acids in feces samples of *Cyp2c*-null mice, h*CYP2C9*, and wild-type mice. Data are presented as the mean ± S. D. (n = 3). N means not detected.

FIGURE 1

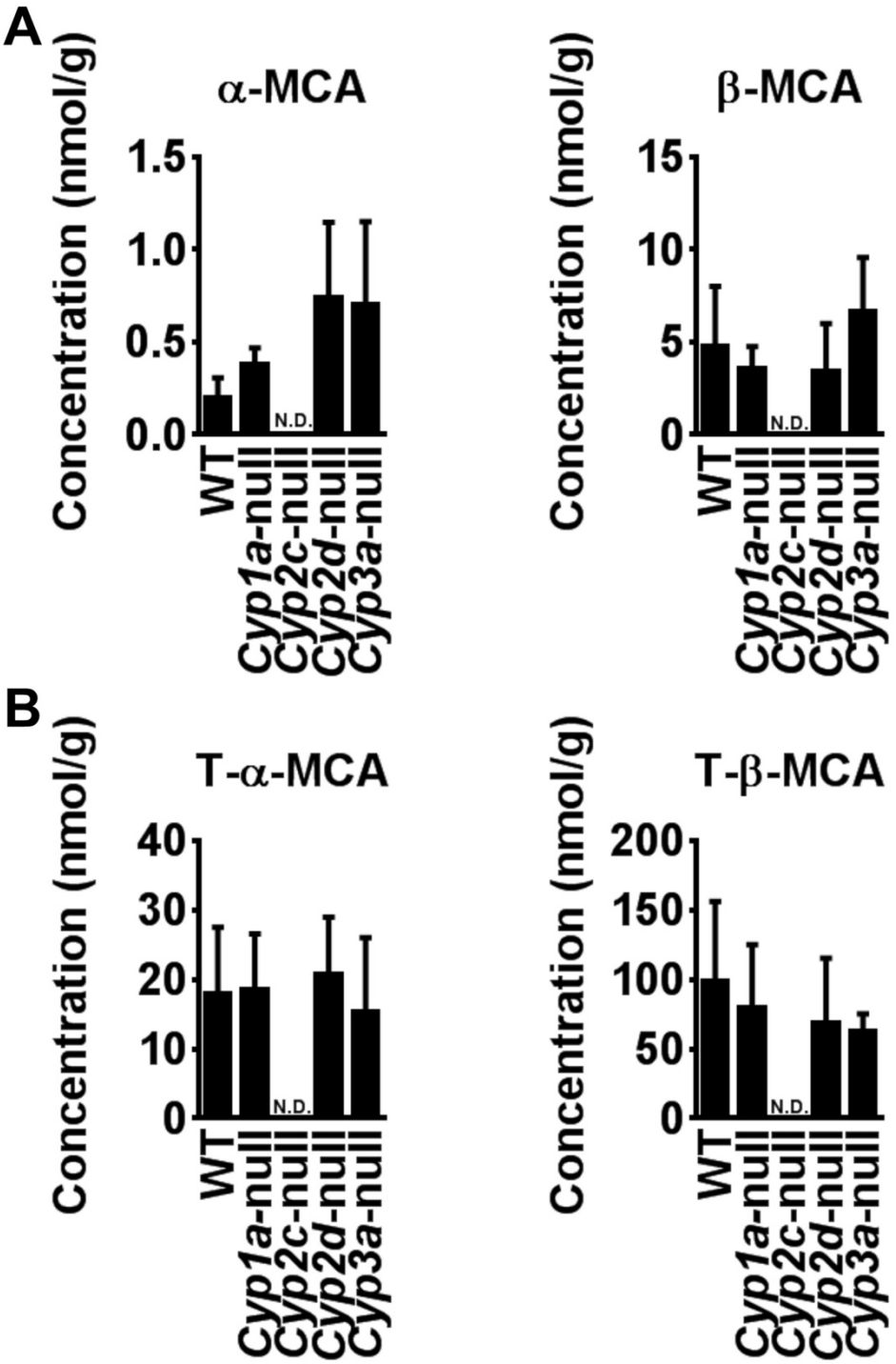

FIGURE 2

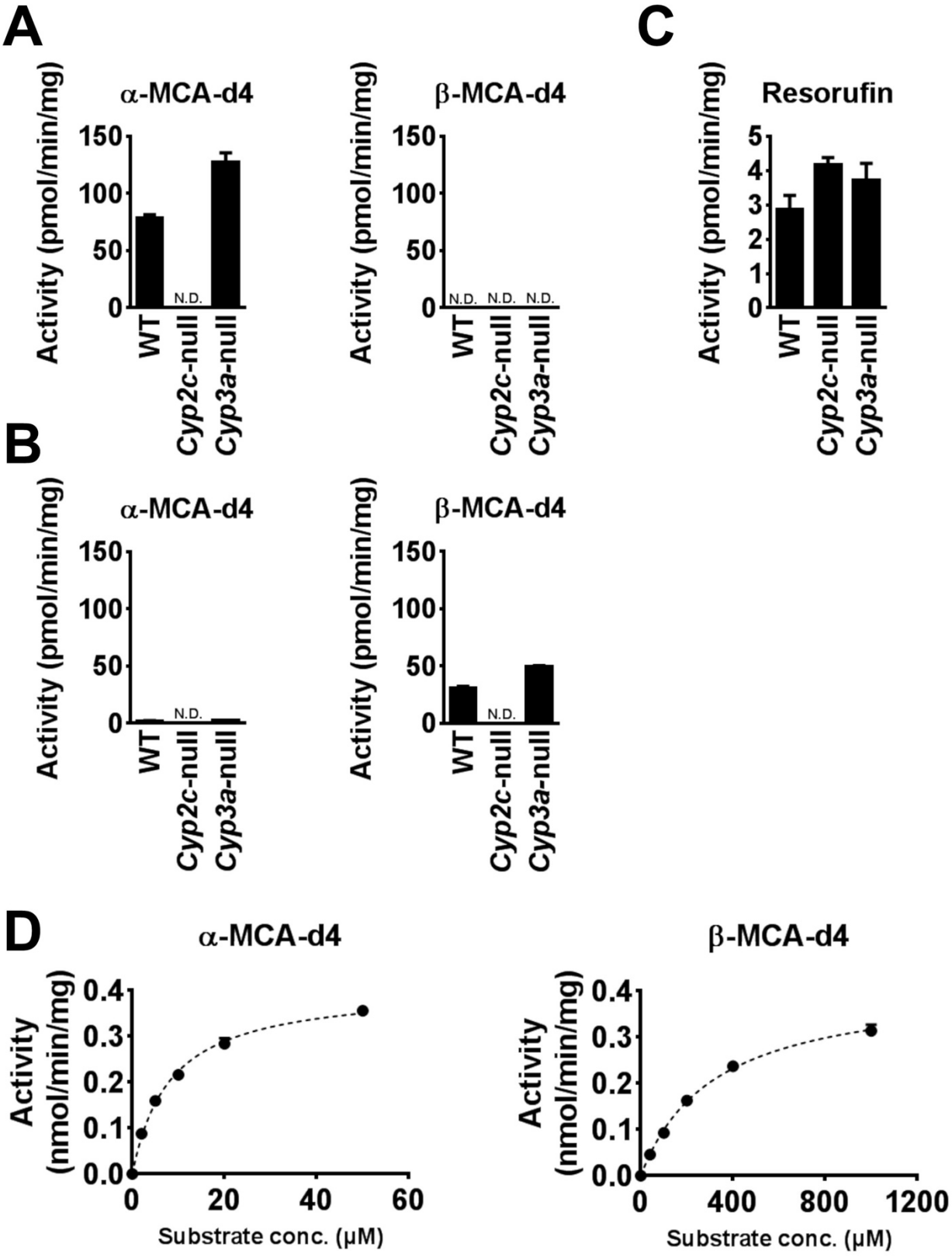

JOURNAL OF LIPID RESEARCH ASBMB

FIGURE 3

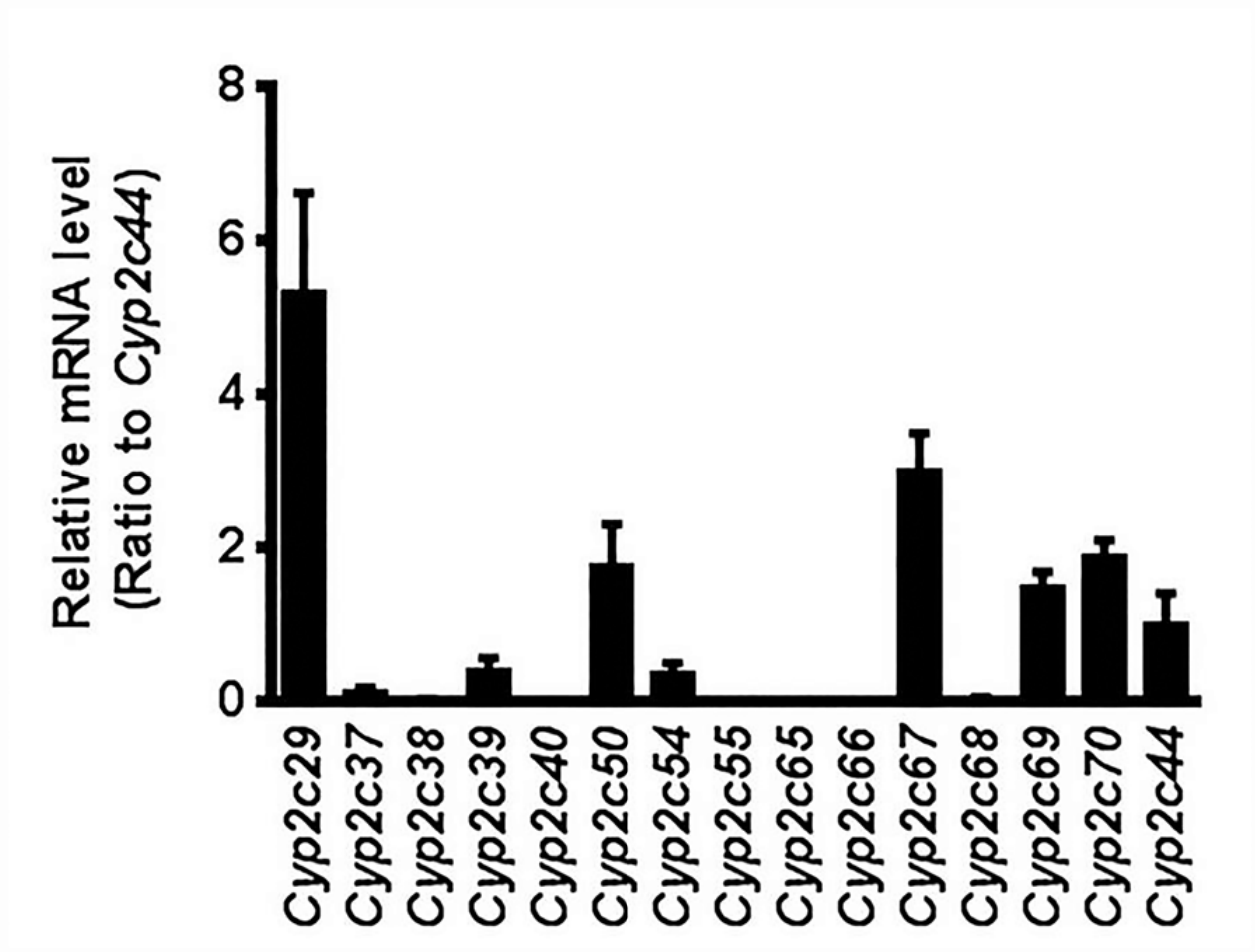

FIGURE 4

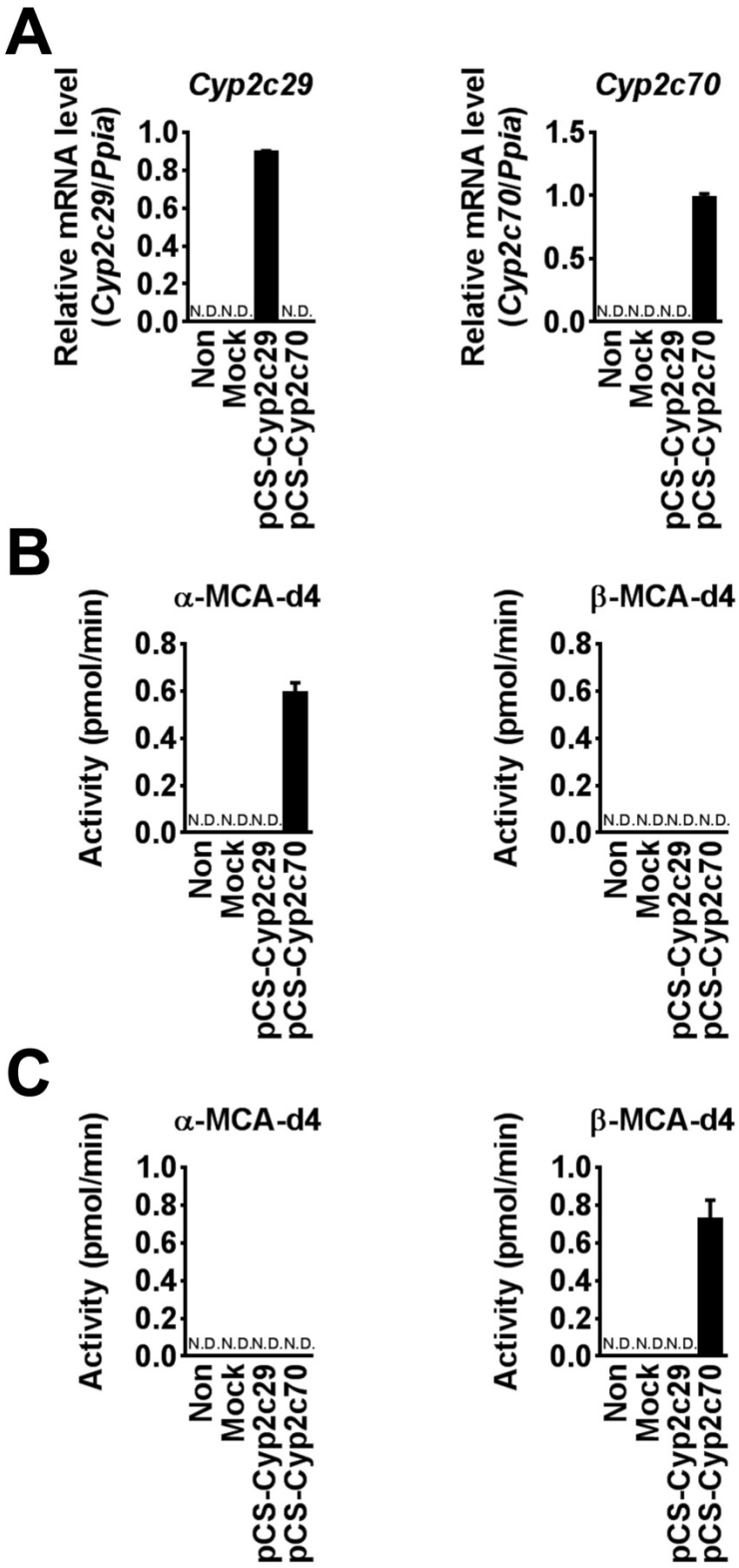

FIGURE 5

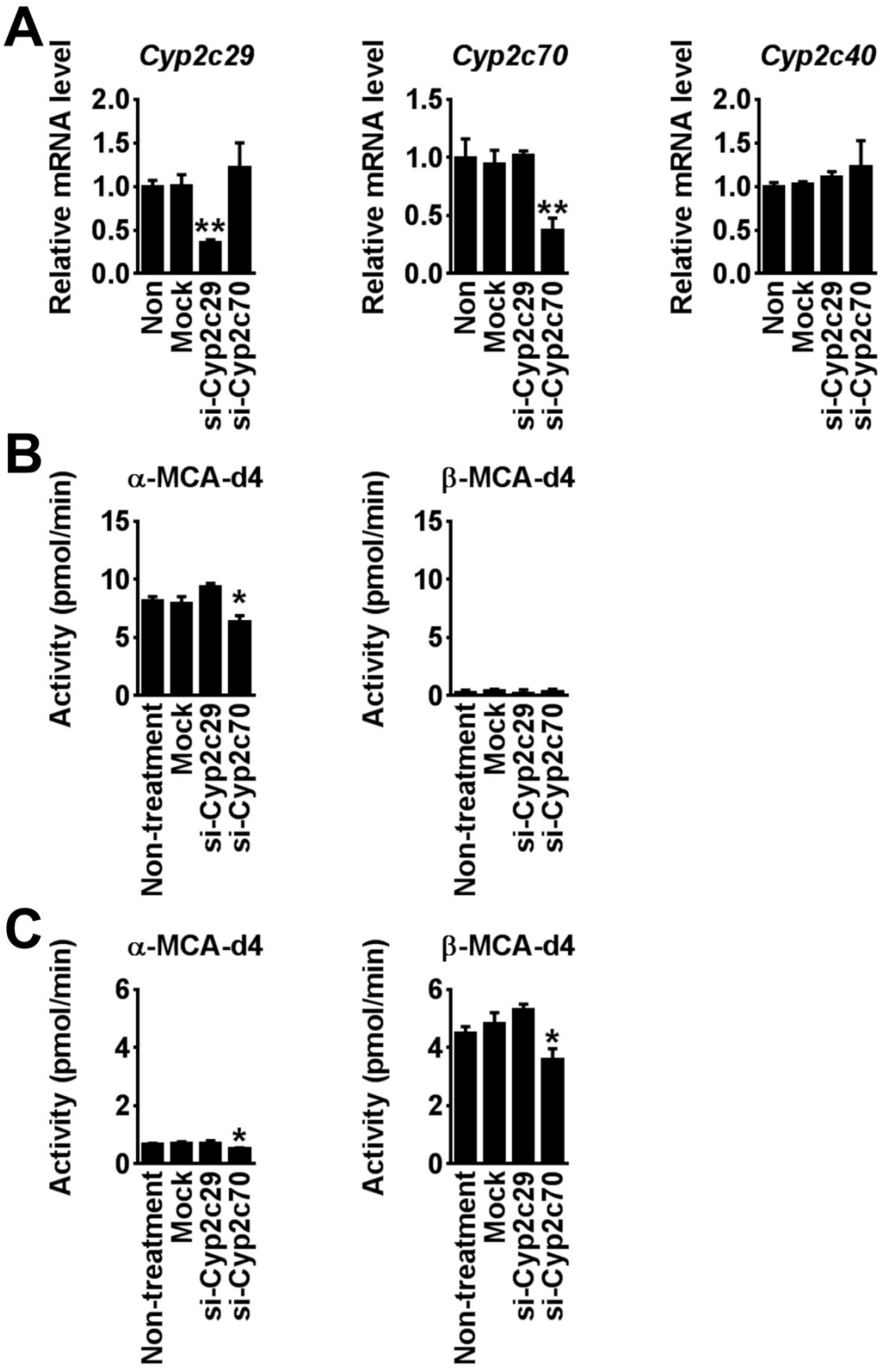

FIGURE 6